

Synthesis and green up-conversion fluorescence of colloidal $\text{La}_{0.78}\text{Yb}_{0.20}\text{Er}_{0.02}\text{F}_3/\text{SiO}_2$ core/shell nanocrystals

Yan Wang^b, Weiping Qin^{a,b,*}, Jisen Zhang^b, Chunyan Cao^b, Jishuang Zhang^b, Ye Jin^b, Peifen Zhu^a, Guodong Wei^a, Guofeng Wang^a, Lili Wang^a

^aState Key Laboratory of Integrated Optoelectronics, College of Electronic Science & Engineering, Jilin University, Changchun 130012, China

^bKey Laboratory of Excited State Processes, Changchun Institute of Optics, Fine Mechanics and Physics, Chinese Academy of Sciences, Changchun 130033, China

Received 2 February 2007; received in revised form 16 May 2007; accepted 28 May 2007

Available online 12 June 2007

Abstract

Water-soluble PVP-stabilized hexagonal-phase $\text{La}_{0.78}\text{Yb}_{0.20}\text{Er}_{0.02}\text{F}_3$ nanocrystals (NCs) were synthesized by hydrothermal method. The NCs were coated with a very thin silica shell, and amino groups were introduced to the surface of silica shells by copolymerization of 3-aminopropyl(triethoxy)silane. The core/shell NCs can be dispersed in ethanol and water to form stable colloidal solution. The transmission electron microscopy (TEM), selected area electron diffraction (SAED), powder X-ray diffraction (XRD), and Fourier transform infrared spectroscopy (FT-IR) were used to characterize the core/shell materials. In addition, the green up-conversion fluorescence mechanism of $\text{La}_{0.78}\text{Yb}_{0.20}\text{Er}_{0.02}\text{F}_3/\text{SiO}_2$ NCs was studied with a 980-nm diode laser as excitation source. The water solubility, small core/shell particles size, and well colloidal stability mean the green up-conversion fluorescence NCs have potential applications in bioassay.

© 2007 Elsevier Inc. All rights reserved.

Keywords: Up-conversion fluorescence; $\text{La}_{0.78}\text{Yb}_{0.20}\text{Er}_{0.02}\text{F}_3/\text{SiO}_2$; Core/shell; Colloidal; Nanocrystals

1. Introduction

Recently, lanthanide-doped up-conversion fluorescence nanocrystals (NCs) [1–6] have attracted much attention due to potential applications as sensitive bio-probes [3,7–9]. The up-conversion fluorescence detection absents auto-fluorescence and reduces light scattering, which results in high sensitivity [10–11], and infrared (IR) or near-infrared (NIR) light are usually used as excitation sources, which can penetrate deep into organisms and reduce photo-bleaching [12,13]. In addition, the different colors of up-converting phosphor can be excited simultaneously with the same IR source (980 nm), which is necessary to

multiplexing. These unique properties make lanthanide up-conversion fluorescence ideal as bio-probes in fluorescence detection of biomolecules.

For lanthanide-doped up-conversion NCs, the selection of host matrix is very important in achieving high efficient up-conversion fluorescence. As a promising host matrix, LaF_3 with low phonon energy has attracted considerable attention in recent years [14–16]. However, applications of LaF_3 NCs in biological systems have been limited due to lacking groups on the surface of the NCs serving as reactive sites for coupling biomolecules. On the other hand, fluoride would be toxic to biological systems. Hence, much work has to be done to modify the surface of NCs. A simple but effective method is to grow a silica shell around the NCs, forming the so-called core–shell structures [17–21]. The silica coating can improve the photostability and biocompatibility of the NCs and the protocol for conjugation of biomolecules to a silica surface is well

*Corresponding author. State Key Laboratory of Integrated Optoelectronics, College of Electronic Science & Engineering, Jilin University, 2699 Qianjin Street, Changchun 130012, China. Fax: +86 431 85168240x8325.
E-mail address: wpqin@jlu.edu.cn (W. Qin).

established [17–19]. However, in many cases, the thickness of the shells is relatively large, which prevents the NCs from using as bio-probes, particularly in fluorescence resonance energy transfer (FRET) process. As we know, the effective distance of FRET is usually lower than 10 nm. Therefore, the size of NCs should not distinctly grow after coated with silica. That is, the thickness of silica shell must be very thin. Furthermore, in order to exploit core/shell NCs peculiar properties and unique biological applications, the NCs should have excellent solubility and stability in polar solvents, particularly, in water.

In this paper, we synthesized 10 nm hexagonal phase $\text{La}_{0.78}\text{Yb}_{0.20}\text{Er}_{0.02}\text{F}_3$ NCs and coated the NCs with 1–2 nm silica shell, as evidenced by TEM images. The free amino groups were introduced by hydrolysis and copolymerization reactions of 3-aminopropyl(triethoxyl)silane (APS), which makes surface bioconjugation of the NCs easy. The $\text{La}_{0.78}\text{Yb}_{0.20}\text{Er}_{0.02}\text{F}_3/\text{SiO}_2$ NCs can be dispersed in ethanol and water and stabilize for 24 h without any visible precipitate. Moreover, the colloidal solutions present green up-conversion fluorescence under a 980-nm excitation from a diode laser, which provides a promising up-conversion NCs for biological applications.

2. Experimental

Rare earth chemicals were obtained from Shanghai Yuelong New Materials Co., Ltd. 3-aminopropyl(triethoxyl)silane (APS, 97%) was obtained from Avocado Research Chemical Ltd. The other chemicals utilized in the synthesis were purchased from Beijing Chemical Corporation and used without further purification. In a typical preparation, 4 mmol $\text{LnNO}_3 \cdot 6\text{H}_2\text{O}$ ($\text{Ln} = \text{La}$ 0.78 mmol, Yb 0.20 mmol, Er 0.02 mmol) and 2.2 g Polyvinylpyrrolidone K-30 (PVP) were dissolved into 40-mL ethylene glycol. The solution was heated to 80 °C until a homogeneous solution was formed. A volume of 40-mL ethylene glycol containing 12 mmol $\text{KF} \cdot 2\text{H}_2\text{O}$ was added dropwise to the above solution. The mixture was agitated for another 30 min and then transferred to four 50-mL autoclaves, sealed, and treated at 160 °C for 16 h. Subsequently, the mixture was allowed to cool to room temperature, and the NCs were separated by centrifugation and washed several times with absolute ethanol, then dried under vacuum at 60 °C overnight.

The procedure for coating silica onto the $\text{La}_{0.78}\text{Yb}_{0.20}\text{Er}_{0.02}\text{F}_3$ NCs was as follows: 0.0897 g $\text{La}_{0.78}\text{Yb}_{0.20}\text{Er}_{0.02}\text{F}_3$ NCs were dispersed in 5-mL ethanol and mixed with 4-mL water and 500 μL ammonia (50%). A volume of 40 μL Tetraethoxysilane (TEOS) dissolved in 8-mL ethanol was then added slowly to the solution under continuous stirring. Then 10 μL 3-aminopropyl(triethoxyl)silane (APS) dissolved in 2-mL ethanol was added dropwise to the solution. The product was isolated by centrifugation and washed with absolute ethanol and water, then dried under vacuum at 60 °C overnight.

The size and morphology of $\text{La}_{0.78}\text{Yb}_{0.20}\text{Er}_{0.02}\text{F}_3$ and $\text{La}_{0.78}\text{Yb}_{0.20}\text{Er}_{0.02}\text{F}_3/\text{SiO}_2$ were characterized by TEM (JEM, 2000EX 200KV). Phase identification was performed via X-ray diffractometry (model Rigaku RU-200b), using nickel-filtered $\text{CuK}\alpha$ radiation ($\lambda = 1.5406 \text{ \AA}$). FT-IR spectra within the range of 4000–400 cm^{-1} were registered by a Bio-Rad FT-IR spectrometer with the KBr pellet technique. The KBr was dried overnight before used. A high-temperature lamp was used to eliminate absorbed water when the KBr/sample was grounded. The samples were analyzed immediately after preparing the pellets. The up-conversion emission spectra were recorded with a Hitachi F-4500 fluorescence spectrometer. An adjustable laser diode (980 nm, 2 W) was used as the excitation source. The up-conversion fluorescence photo of colloidal solution was taken with a digital camera.

3. Results and discussion

The powder X-ray diffraction (XRD) results of the $\text{La}_{0.78}\text{Yb}_{0.20}\text{Er}_{0.02}\text{F}_3$ and $\text{La}_{0.78}\text{Yb}_{0.20}\text{Er}_{0.02}\text{F}_3/\text{SiO}_2$ NCs are shown in Fig. 1. The peak positions and intensity agree well with the data reported in the JCPDS standard card (84-0691) of pure hexagonal LaF_3 crystals [22–24]. No impurity can be identified from the XRD pattern, which suggests that our synthesis is a promising method to prepare pure hexagonal phase LaF_3 . As we know, the nanocrystallite size can be estimated from the Scherrer formula, $D = 0.941\lambda/\beta \cos \theta$, where D is the average grain size, λ is the X-ray wavelength (0.15405 nm), θ is the diffraction angle and β is full-width at half-maximum (FWHM) of an observed peak. By applying the Scherrer formula to the FWHM of the (111) diffraction peak, the mean particle sizes of $\text{La}_{0.78}\text{Yb}_{0.20}\text{Er}_{0.02}\text{F}_3$ and $\text{La}_{0.78}\text{Yb}_{0.20}\text{Er}_{0.02}\text{F}_3/\text{SiO}_2$ NCs could be calculated as 7.8 and 8.0 nm, respectively. The small grain size results in the broadening of the XRD peaks of these two NCs.

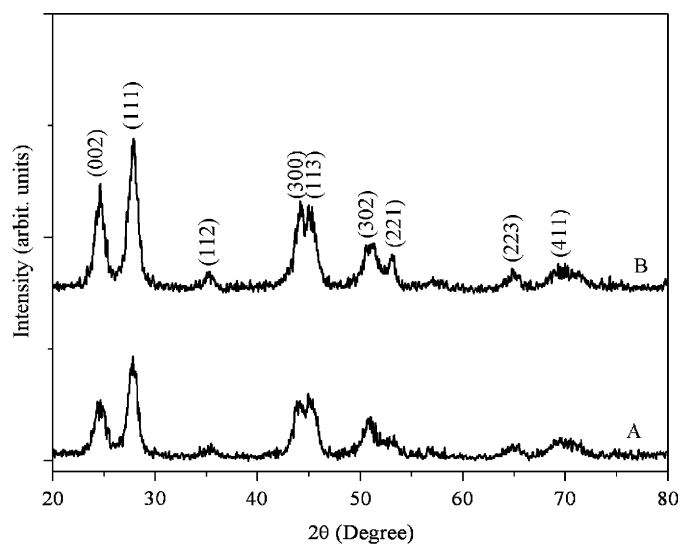


Fig. 1. Powder X-ray diffraction (XRD) patterns of $\text{La}_{0.78}\text{Yb}_{0.20}\text{Er}_{0.02}\text{F}_3$ (A) and $\text{La}_{0.78}\text{Yb}_{0.20}\text{Er}_{0.02}\text{F}_3/\text{SiO}_2$ NCs (B).

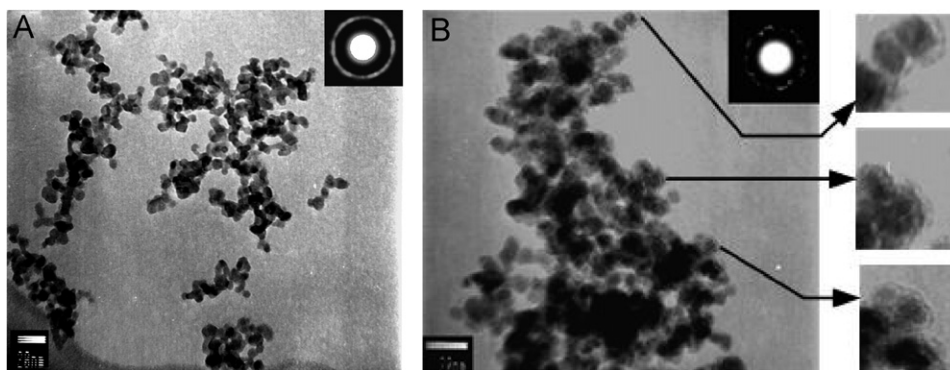


Fig. 2. TEM images of $\text{La}_{0.78}\text{Yb}_{0.20}\text{Er}_{0.02}\text{F}_3$ (A) and $\text{La}_{0.78}\text{Yb}_{0.20}\text{Er}_{0.02}\text{F}_3/\text{SiO}_2$ NCs (B). Insets: The electronic diffraction patterns of $\text{La}_{0.78}\text{Yb}_{0.20}\text{Er}_{0.02}\text{F}_3$ and $\text{La}_{0.78}\text{Yb}_{0.20}\text{Er}_{0.02}\text{F}_3/\text{SiO}_2$ NCs, respectively (the scale bar is 20 nm).

Figs. 2A and B show TEM images of the $\text{La}_{0.78}\text{Yb}_{0.20}\text{Er}_{0.02}\text{F}_3$ and $\text{La}_{0.78}\text{Yb}_{0.20}\text{Er}_{0.02}\text{F}_3/\text{SiO}_2$ NCs, respectively. From Fig. 2A, we can see that the crystals are nearly spherical in shape and relatively uniform in size with an average size of about 10 nm, which agrees well with XRD results. TEM image of the silica-coated $\text{La}_{0.78}\text{Yb}_{0.20}\text{Er}_{0.02}\text{F}_3$ NCs shows that the thickness of the silica shell is about 1–2 nm, which is further indicated by the magnified images of Fig. 2B. Owing to adding a small amount of TEOS and APS, the silica-coated NCs still retain 10-nm average size. The small grain size makes core/shell NCs promising as bio-probes. The SAED patterns of $\text{La}_{0.78}\text{Yb}_{0.20}\text{Er}_{0.02}\text{F}_3$ and $\text{La}_{0.78}\text{Yb}_{0.20}\text{Er}_{0.02}\text{F}_3/\text{SiO}_2$ NCs (insets in Figs. 2A and B, respectively) also confirm that the resulting NCs are well crystallized.

Fig. 3 shows infrared transmission spectra of $\text{La}_{0.78}\text{Yb}_{0.20}\text{Er}_{0.02}\text{F}_3$ and $\text{La}_{0.78}\text{Yb}_{0.20}\text{Er}_{0.02}\text{F}_3/\text{SiO}_2$ NCs. In the FT-IR spectrum of $\text{La}_{0.78}\text{Yb}_{0.20}\text{Er}_{0.02}\text{F}_3$ NCs, the broad absorption band located at 3400 cm^{-1} could be assigned to $-\text{OH}$ groups from the absorbed water. The peaks at 2930 and 1380 cm^{-1} corresponding to the stretching and bending modes of $-\text{CH}_2$ groups, the double peaks at 1088 – 1050 cm^{-1} corresponding to the C–N stretching modes, and the characteristic peak at 1640 cm^{-1} corresponding to the C=O stretching vibrations indicate the presence of PVP on the surface of the NCs as a capping ligand [25,26]. PVP is an amphiphilic surfactant, which can make the NCs dispersible in water and organic solvents [27]. Furthermore, its pyrrolidone groups can coordinate with lanthanide ions, as reported by different authors [28–30]. In regard to the silica-coated NCs, aside from the presence of the characteristic absorption bands of PVP, the strong absorption peak around 1050 cm^{-1} is attributed to Si–O–Si asymmetrical stretching vibration. The symmetric stretching vibration of Si–O–Si at 782 cm^{-1} also appears in the spectrum of silica-coated NCs. The absorption bands in the region of 3700 – 3000 cm^{-1} are based on stretching vibration of $-\text{NH}_2$ groups from silica shells and $-\text{OH}$ groups from the absorbed water. The IR peaks at 1530 cm^{-1} corresponding to the bending mode of N–H band further indicates that the surface of silica shells is

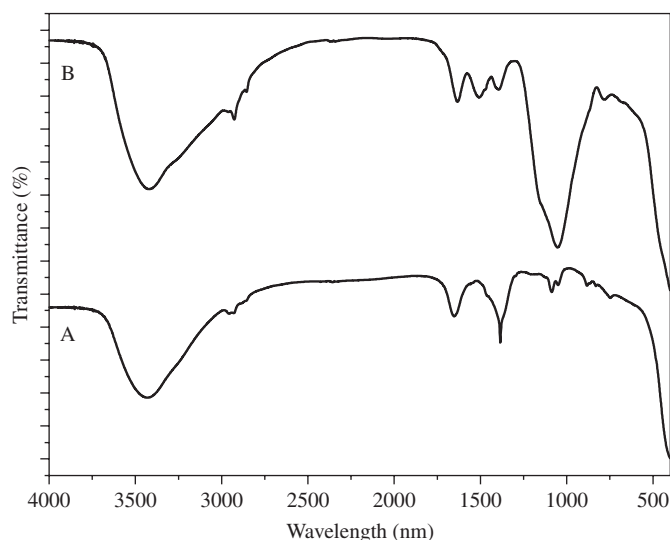


Fig. 3. FT-IR spectra of $\text{La}_{0.78}\text{Yb}_{0.20}\text{Er}_{0.02}\text{F}_3$ (A) and $\text{La}_{0.78}\text{Yb}_{0.20}\text{Er}_{0.02}\text{F}_3/\text{SiO}_2$ NCs (B).



Fig. 4. Photographs of $\text{La}_{0.78}\text{Yb}_{0.20}\text{Er}_{0.02}\text{F}_3/\text{SiO}_2$ NCs dispersed in ethanol (left) and in water (right) with the concentration of 5 mg/mL.

modified with amino groups by hydrolysis and copolymerization reactions of APS, which makes surface bioconjugation of the NCs easy.

Fig. 4 demonstrates that the $\text{La}_{0.78}\text{Yb}_{0.20}\text{Er}_{0.02}\text{F}_3/\text{SiO}_2$ NCs can easily disperse in the polar solvents ethanol and water to form stable colloidal solution. The $\text{La}_{0.78}\text{Yb}_{0.20}\text{Er}_{0.02}\text{F}_3/\text{SiO}_2$ NCs colloidal solution could be stable for 24 h without aggregates observed in the bottom of the colloidal suspension. The well dispersivity and stability of the sample in ethanol and water are very important to explore the bio-applications of core/shell sample.

The room temperature up-conversion spectrum of $\text{La}_{0.78}\text{Yb}_{0.20}\text{Er}_{0.02}\text{F}_3/\text{SiO}_2$ colloidal solution in ethanol is presented in Fig. 5. Under 980-nm excitation, four emission peaks in the visible region are assigned to ${}^2\text{H}_{9/2} \rightarrow {}^4\text{I}_{15/2}$ (408 nm), ${}^2\text{H}_{11/2} \rightarrow {}^4\text{I}_{15/2}$ (520 nm), ${}^4\text{S}_{3/2} \rightarrow {}^4\text{I}_{15/2}$ (540 nm) and ${}^4\text{F}_{9/2} \rightarrow {}^4\text{I}_{15/2}$ (650 nm) transitions of Er^{3+} ions, respectively [1,31]. Obviously, the green emission is dominant in the up-conversion fluorescence spectrum of the $\text{La}_{0.78}\text{Yb}_{0.20}\text{Er}_{0.02}\text{F}_3/\text{SiO}_2$ colloidal solution. Inset of Fig. 5 gives the green up-conversion fluorescence photograph of $\text{La}_{0.78}\text{Yb}_{0.20}\text{Er}_{0.02}\text{F}_3/\text{SiO}_2$ colloidal solution excited under a 980-nm diode laser with a pump power density of 130 W/cm^2 , which suggests that the $\text{La}_{0.78}\text{Yb}_{0.20}\text{Er}_{0.02}\text{F}_3/\text{SiO}_2$ is a promising colloidal solution for green labeling. Since the luminescence of lanthanide ions is efficiently quenched by the high-energy O–H and N–H vibrations from the absorption water and surface amino groups, lanthanide ions on the crystal surface are not likely to show IR-to-green up-conversion. Therefore, the observed up-conversion fluorescence should emit from the Ln^{3+} ($\text{Ln}^{3+} = \text{Yb}^{3+}, \text{Er}^{3+}$) ions replacing the La^{3+} ions inside the NCs. In the next discussion, we focus our attention on the dominant green emissions. For unsaturated up-conversion emission intensity, I_s , is proportional to I^n , where I is the intensity of the excitation light and the integer n is the number of photons absorbed in one up-conversion emission process. In Fig. 6, we give the intensity

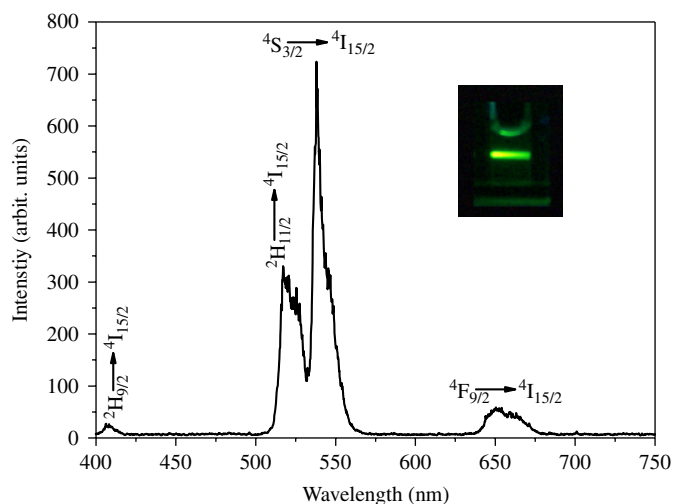


Fig. 5. Up-conversion emission spectrum of $\text{La}_{0.78}\text{Yb}_{0.20}\text{Er}_{0.02}\text{F}_3/\text{SiO}_2$ colloidal solution excited at 980 nm. Inset shows the green up-conversion fluorescence of 200- μL $\text{La}_{0.78}\text{Yb}_{0.20}\text{Er}_{0.02}\text{F}_3/\text{SiO}_2$ ethanol solution with a 5-mg/mL concentration.

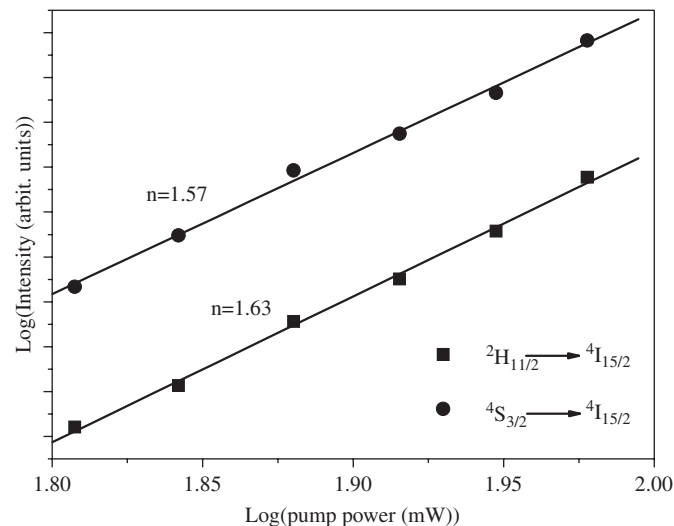


Fig. 6. Intensity dependences of the green up-converted fluorescence of $\text{La}_{0.78}\text{Yb}_{0.20}\text{Er}_{0.02}\text{F}_3/\text{SiO}_2$ on the pump power excitation at 980 nm.

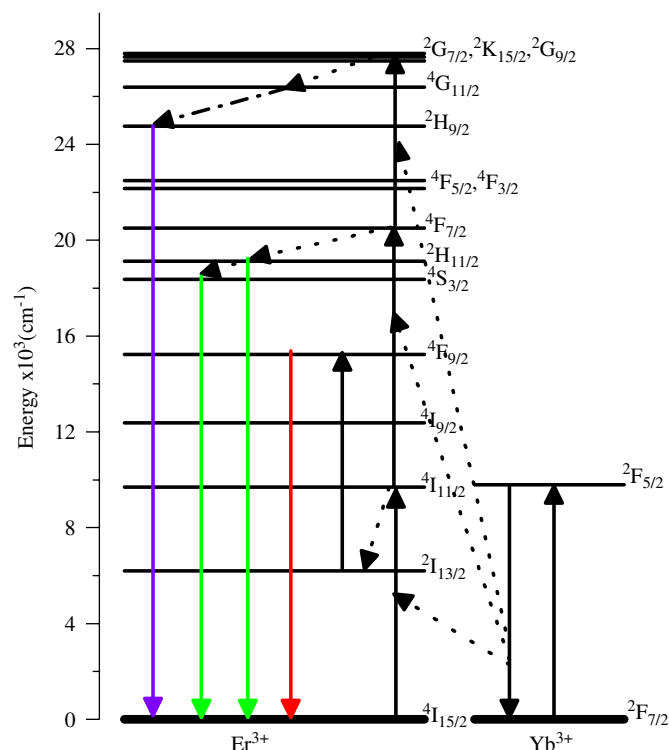


Fig. 7. Schematic diagram of Yb^{3+} -sensitized Er^{3+} up-conversion in $\text{La}_{0.78}\text{Yb}_{0.20}\text{Er}_{0.02}\text{F}_3/\text{SiO}_2$ NCs under 980-nm excitation.

dependences of the green up-converted fluorescence on the pump power at 980-nm excitation. The number of photons of 980-nm IR light required to excite the green up-conversion emissions was determined from the slope of the line of the bi-logarithmic plots, as shown in Fig. 6. The slopes of $\log(I_s)$ versus $\log(I)$ are 1.57 and 1.63 (peaks centered at 540 and 520 nm, respectively) for the $\text{La}_{0.78}\text{Yb}_{0.20}\text{Er}_{0.02}\text{F}_3/\text{SiO}_2$ colloidal solution, and therefore the green up-conversion emissions in Er^{3+} ions occur via a

two-photon process. Infrared to green up-conversion emissions in $\text{Yb}^{3+}\text{--Er}^{3+}$ codoped system has been widely investigated [15,31]. Fig. 7 gives the schematic energy level diagrams of up-conversion excitation and visible emission for the $\text{Yb}^{3+}/\text{Er}^{3+}$. As indicated by the arrows, Yb^{3+} ion was excited from the ground state $^2F_{7/2}$ to the excited state $^2F_{5/2}$ by an infrared (980 nm) photon. The Yb^{3+} ion may transfer the energy to the Er^{3+} ion, which can promote an electron from $^4I_{15/2}$ to $^4I_{11/2}$ state, and if the latter is already populated, the electron may transit from the $^4I_{11/2}$ to the $^4F_{7/2}$ states. Subsequently, nonradiative relaxations could populate the $^2H_{11/2}$ and $^4S_{3/2}$ states, which are the emitting levels for the green fluorescence. Therefore, the green up-conversion luminescence is duo to two-photon processes. For the violet emission, there are two processes in populating the state $^2H_{9/2}$: (1) energy transfer $^2F_{5/2} \rightarrow ^2F_{7/2}$ (Yb^{3+}): $^4F_{9/2} \rightarrow ^2H_{9/2}$ (Er^{3+}); and (2) energy transfer $^2F_{5/2} \rightarrow ^2F_{7/2}$ (Yb^{3+}): $^4S_{3/2} \rightarrow ^2G_{7/2}$ (Er^{3+}), followed by fast cascading relaxation to the $^4G_{11/2}$ and $^2H_{9/2}$ states.

4. Conclusion

In conclusion, we synthesized $\text{La}_{0.78}\text{Yb}_{0.20}\text{Er}_{0.02}\text{F}_3$ and $\text{La}_{0.78}\text{Yb}_{0.20}\text{Er}_{0.02}\text{F}_3/\text{SiO}_2$ NCs using simple methods. XRD analysis showed that the products were single hexagonal phase. TEM images showed the $\text{La}_{0.78}\text{Yb}_{0.20}\text{Er}_{0.02}\text{F}_3$ NCs have an average size of 10 nm, and $\text{La}_{0.78}\text{Yb}_{0.20}\text{Er}_{0.02}\text{F}_3/\text{SiO}_2$ NCs have very thin silica shells. Moreover, free amino groups are introduced to the surface of silica shells by copolymerization of APS. The core/shell NCs can disperse in ethanol and water to form stable colloidal solutions and the colloidal solutions exhibit green up-conversion fluorescence under 980-nm excitation. Excitation of $\text{La}_{0.78}\text{Yb}_{0.20}\text{Er}_{0.02}\text{F}_3/\text{SiO}_2$ sample with 980 nm populates the $^4F_{7/2}$ state of Er^{3+} ions via two successive energy transfer from the Yb^{3+} ions and yields intense green up-conversion luminescence. The core/shell NCs have potential applications in bioimaging and biolabeling.

Acknowledgments

The authors thank the National Science Foundation of China for supporting this work. (Grant Numbers are 10474096 and 50672030).

References

- [1] S. Heer, K. Kompe, H.U. Gudel, M. Haase, *Adv. Mater.* 16 (2004) 2102.
- [2] J.H. Zeng, J. Su, Z.H. Li, R.X. Yan, Y.D. Li, *Adv. Mater.* 17 (2005) 2119.
- [3] G.S. Yi, H.C. Lu, S.Y. Zhao, G. Yue, W.J. Yang, D.P. Chen, L.H. Guo, *NanoLetters* 4 (2004) 2191.
- [4] G.S. Yi, G.M. Chow, *Adv. Funct. Mater.* 16 (2006) 2324.
- [5] H.X. Mai, Y.W. Zhang, R. Si, Z.G. Yan, L.D. Sun, L.P. You, C.H. Yan, *J. Am. Chem. Soc.* 128 (2006) 6426.
- [6] J.C. Boyer, F. Vetrone, L.A. Cuccia, J.A. Capobianco, *J. Am. Chem. Soc.* 128 (2006) 7444.
- [7] F. van de Rijcke, H. Zijlmans, S. Li, T. Vail, A.K. Raap, R.S. Niedbala, H.J. Tanke, *Nat. Biotechnol.* 19 (2001) 273.
- [8] S.F. Lim, R. Riehn, W.S. Ryu, N. Khanarian, C.K. Tung, D. Tank, R.H. Austin, *NanoLetters* 6 (2006) 169.
- [9] L.Y. Wang, Y.D. Li, *Chem. Commun.* 24 (2006) 2557.
- [10] H.J.M.A. Zijlmans, J. Bonnet, J. Burton, K. Kardos, T. Vail, R.S. Niedbala, H.J. Tanke, *Anal. Biochem.* 267 (1999) 30.
- [11] J.A. Feijo, N. Moreno, *Protoplasma* 223 (2004) 1.
- [12] R.W. Waynant, I.K. Ilev, I. Gannot, *Philos. Trans. R. Soc. London Ser. A* 359 (2001) 635.
- [13] W.C.W. Chan, S.M. Nie, *Science* 281 (1998) 2016.
- [14] J.W. Stouwdam, F.C.J.M. van Veggel, *NanoLetters* 2 (2002) 733.
- [15] G.J.H. De, W.P. Qin, J.S. Zhang, D. Zhao, *Chem. Lett.* 34 (2005) 914.
- [16] S. Sivakumar, P.R. Diamente, F.C.J.M. van Veggel, *Chem. Eur. J.* 12 (2006) 5878.
- [17] M.Q. Tan, Z.Q. Ye, G.L. Wang, J.L. Yuan, *Chem. Mater.* 16 (2004) 2494.
- [18] X.J. Zhao, P.R. Bagwe, W.H. Tan, *Adv. Mater.* 16 (2004) 173.
- [19] S. Santra, P. Zhang, K.M. Wang, R. Tapeç, W.H. Tan, *Anal. Chem.* 73 (2001) 4988.
- [20] L. Wang, C.Y. Yang, W.H. Tan, *NanoLetters* 5 (2005) 37.
- [21] X.J. Zhang, R. Tapeç-Dytioco, W.H. Tan, *J. Am. Chem. Soc.* 125 (2003) 11474.
- [22] X. Wang, J. Zhuang, Q. Peng, Y.D. Li, *Inorg. Chem.* 45 (2006) 6661.
- [23] G.S. Yi, G.M. Chow, *J. Mater. Chem.* 15 (2005) 4460.
- [24] M.M. Lage, A. Righi, F.M. Matinaga, J.-Y. Gesland, R.L. Moreira, *J. Phys.: Condens. Matter* 16 (2004) 3207.
- [25] Y. Gao, L. Song, P. Jiang, L.F. Liu, X.Q. Yan, Z.P. Zhou, D.F. Liu, J.X. Wang, H.J. Yuan, Z.X. Zhang, X.W. Zhao, X.Y. Dou, W.Y. Zhou, G. Wang, S.S. Xie, H.Y. Chen, J.Q. Li, *J. Cryst. Growth* 276 (2005) 606.
- [26] M.H. Liu, X.P. Yan, H.F. Liu, W.Y. Yu, *React. Funct. Polym.* 44 (2000) 55.
- [27] Y. Yang, J.R. Li, J. Mu, H.L. Rong, L. Jiang, *Nanotechnology* 17 (2006) 461.
- [28] Z.Q. Li, Y. Zhang, *Angew. Chem. Int. Ed.* 45 (2006) 7732.
- [29] D.M.L. Goodgame, D.J. Williams, R.E.P. Winpenny, *Angew. Chem. Int. Ed. Engl.* 27 (1988) 261.
- [30] Q. Li, T. Li, J.G. Wu, *J. Phys. Chem. B* 105 (2001) 12293.
- [31] G.S. Qin, W.P. Qin, S.H. Huang, C.F. Wu, D. Zhao, B.J. Chen, S.Z. Lu, E. Shulin, *J. Appl. Phys.* 92 (2002) 6936.